

Spectroscopic and magnetic mirages of impurities in nanoscopic systems

K. Hallberg, A. Correa, and C. A. Balseiro

Instituto Balseiro and Centro Atómico Bariloche, Comisión Nacional de Energía Atómica, 8400 San Carlos de Bariloche, Argentina.

(November 13, 2018)

We present exact results for magnetic impurities in nanoscopic systems with focusing properties. We analyze the spectroscopic and magnetic properties of Kondo, intermediate valence and magnetic impurities on a sphere with a metallic surface. Exact calculations show the occurrence of spectroscopic and magnetic mirages at the antipodes of the impurity location. Comparison with calculations performed using effective models validates previous calculations of spectroscopic mirages. Our results can be extended to other systems with focusing properties like quantum corrals.

PACS numbers: 72.15.Qm, 73.22.-f

Interference of electron wave-functions is a common phenomena in condensed matter physics which leads to a plethora of effects. Some examples are the formation of energy bands in crystals, the Friedel oscillations in the screening of charged impurities or the Aharonov-Bohm effect in mesoscopic circuits. Up to now, due to technological difficulties, it was not possible to design and build devices that focus electron wave-functions to artificially create images in a metal. In a recent and notorious experiment, Manoharan et al.¹ were able to project the image of a Kondo impurity to a remote location. The device used in this experiment is an elliptical quantum corral on a Cu surface. A Co atom on an open Cu surface behaves as a Kondo impurity and generates a characteristic spectroscopic signature.^{2,3} This signature can be observed by measuring the tunneling current to a scanning tunneling microscope (STM) tip placed at the vicinity of the impurity. The signal disappears when the tip is moved away of the Co impurity a distance of the order of 10 Å. When a Co atom is placed at one of the foci of the elliptic corral, the Kondo signature is not only observed when the STM tip is placed close to the impurity but also when it is located at the empty focus of the corral indicating the coherent refocusing of the electronic structure from one focus to the other.

These experiments triggered a number of theoretical works where the electronic image projection in quantum corrals is analyzed.⁴⁻⁸ All calculations incorporate the Kondo effect in a phenomenological way, either by including a Kondo resonance at the Fermi energy or adding a phase shift to the conduction electrons. The quantum mirages so obtained show that in order to reproduce the spectroscopic properties at the empty focus, correlations do not play an essential role, they only provide the signature of the impurity at the Fermi level where the STM experiment probes the local density of electronic states. The Kondo nature of the Co impurity is relevant only to generate a resonance at the Fermi level. A complete many body theory is still lacking and it is of central importance in order to understand some aspects of the problem. There are still many open questions particularly concerning the spin dynamics in these systems: While in the vicinity of the impurity, conduction electron spins are

screening the Co spin, are spins at the empty focus fluctuating coherently with the impurity spin? Moreover, in the presence of a magnetic non-Kondo impurity that couples ferromagnetically with conduction electrons placed at one focus, is there a magnetic mirage at the empty focus?

The aim of this work is to present a many body calculation of impurities in nanoscopic systems with focusing properties and analyze local density of states at the Fermi level and spin correlations. The calculation is performed by exact diagonalization in small clusters using the Lanczos algorithm^{9,10}. The elliptic corral is not the only geometry with focusing properties, other examples are two mutually facing parabolas at a Cu surface or a thin metallic film covering a rugby ball. In the latter case, an impurity placed at one tip generates a mirage at the other. A particular case of this geometry is a sphere with a metallic surface where any point can be defined as a focus and the mirage is formed at the opposite point: given a point that defines a pole, all meridians cross at the other pole being the “optical” length of all of them the same. The main difference between these geometries is the degeneracy of the one electron states, however a deep understanding of the refocusing properties in one of them will shed some light into all the others.

We analyze the case of the sphere that is the simplest case and is appropriate for exact diagonalization. Conduction electrons are confined at the surface of a sphere of radius R , the electron coordinates are the angles (θ, φ) and a Kondo impurity is placed at $\theta = 0$. The Anderson Hamiltonian reads¹¹:

$$H = \sum_{l,m,\sigma} \varepsilon_l c_{lm\sigma}^\dagger c_{lm\sigma} + \sum_{\sigma} E_d d_{\sigma}^\dagger d_{\sigma} + U d_{\uparrow}^\dagger d_{\uparrow} d_{\downarrow}^\dagger d_{\downarrow} + \sum_{l,\sigma} V_l (c_{l0\sigma}^\dagger d_{\sigma} + d_{\sigma}^\dagger c_{l0\sigma}) \quad (1)$$

where $c_{lm\sigma}^\dagger$ creates an electron with quantum numbers l , m, σ corresponding to the total angular momentum, the z -component of the angular momentum and the spin respectively and with energy $\varepsilon_l = \hbar^2 l(l+1)/2mR^2$, the operator d_{σ}^\dagger creates an electron with spin σ at the impurity orbital with energy E_d and Coulomb repulsion U . The

last term describes the hybridization with $V_l = VY_{l0}(0, 0)$ where $Y_{lm}(\theta, \varphi)$ is the spherical harmonic. For an impurity at the pole ($\theta = 0$), only the $m = 0$ states are hybridized with the impurity orbital. In the summation over l we take a cutoff l_{\max} to avoid including wave functions oscillating with a characteristic wave length shorter than a typical interatomic distance a , $((a/R)l_{\max} \simeq 1)$. In what follows we refer to the impurity site ($\theta = 0$) as the occupied focus and to the point $\theta = \pi$ as the empty focus. Energies are taken in units of $\hbar^2/2mR^2$ and we consider a very large on-site Coulomb repulsion U .

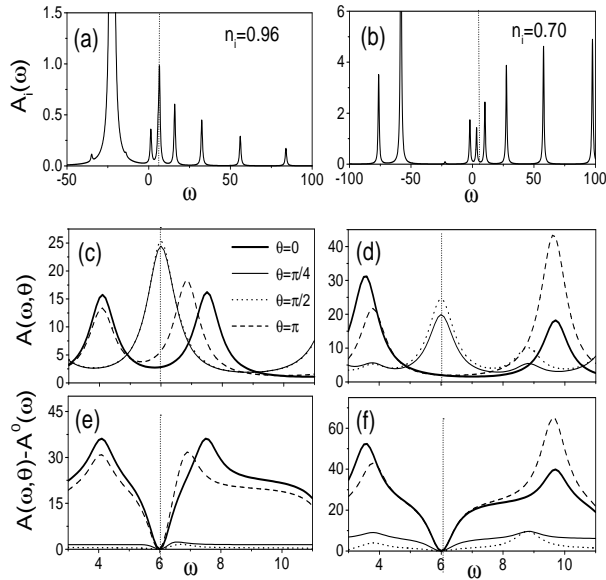


FIG. 1. Spectral density for $E_d = -20$ and two values of the hybridization: $V/4\pi = 1$ ((a), (c), (e)) and $V/4\pi = 5$ ((b), (d), (f)). From top to bottom: impurity spectral density, conduction electrons spectral density for different angles in an expanded scale around ε_F and conduction electrons spectral energy difference with and without impurity. In (e) and (f) curves have been shifted to coincide at ε_F . The Fermi energy is indicated with a vertical dotted line.

We first present exact numerical results for the local density of states for a system with $l_{\max} = 10$ and 14 electrons. In Fig.(1) the impurity spectral density is shown for different values of the parameters (a Lorentzian width of 0.5 is taken). A small hybridization V corresponds to the Kondo regime with an average number of electrons in the impurity orbital $\langle n_d \rangle$ close to one. For the parameters of Fig. (1a) we obtain $\langle n_d \rangle = 0.961$ and the impurity spectral density $A_i(\omega)$ shows a large peak at an energy close to the impurity energy E_d and a number of small peaks at the band energies. Within the band, the dominant peak coincides with the Fermi energy ε_F

and represents the Kondo resonance. A large hybridization ($V > |E_d|$) reduces the number of electrons in the impurity orbital and for the parameters of Fig (1b) we obtain $\langle n_d \rangle = 0.705$ corresponding to an intermediate valence (IV) regime. In this case $A_i(\omega)$ shows a large amplitude at the band energies and does not present a dominant Kondo peak. The conduction electron spectral density $A(\omega, \theta)$ is shown also in Fig. (1) for different values of the angle θ . At the impurity focus, the conduction electron spectral density presents a pseudogap, both for the Kondo and IV regimes (Figs (1c) and (1d)). As θ increases the pseudogap is filled and at the equator ($\theta = \pi/2$) the local density of states resembles the unperturbed density of states. As θ approaches π , the empty focus, a clear mirage of the impurity is obtained both for small and large V . In this simple geometry, the states that fill the pseudogap for $\theta \neq 0, \pi$ correspond to the states with $m \neq 0$. For a better comparison, in Figs. (1e) and (1f) we present the difference $\delta A(\omega, \theta) = A(\omega, \theta) - A^0(\omega, \theta)$ of the conduction electrons spectral density with and without the impurity. This is a typical result when the Fermi energy coincides with one of the non-interacting one-electron levels. When the Fermi energy lies between two conduction energy levels *i.e.* when there is a closed shell in the sphere, the Kondo peak is not observed and the conduction electron spectral density shows a small dependence with θ . These results qualitatively reproduce the experimental observations in the quantum corral where the mirage is observed only for system sizes such that a confined one-electron state lies close to the Fermi energy.¹

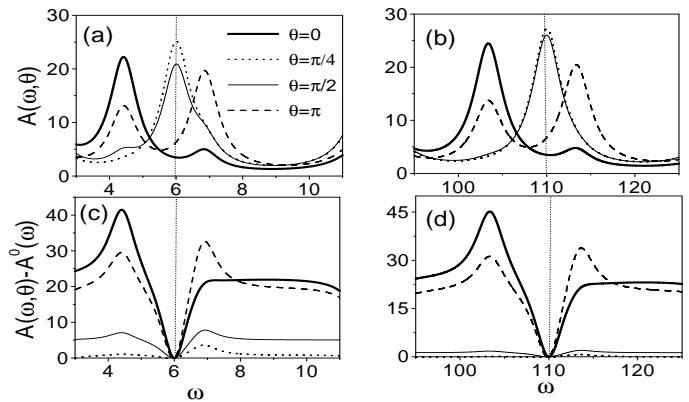


FIG. 2. Conduction electron spectral densities and spectral density difference for an effective resonant level at ε_F . A small system as in Fig.(1) ((a), (c)) and a large system with $l_{\max} = 50$ and 220 electrons ((b), (d)).

The low energy spectrum ($\omega \approx \varepsilon_F$) obtained for the Kondo impurity can be mimicked by representing the Kondo resonance as an uncorrelated resonant level at the Fermi energy, which is precisely the spirit of some previous calculations where the impurity propagator is not fully self-consistently evaluated⁵. A simple calculation

using Hamiltonian (1) with $E_d = \varepsilon_F$, $U = 0$ and a small effective hybridization V gives the results of Fig. (2): for a small system the spectral density for $\omega \approx \varepsilon_F$ qualitatively reproduce the exact results of Figure (1). Due to the simple structure of the one electron wave functions on a sphere it is clear that, although the structure of the difference $\delta A(\omega, \theta)$ on the two foci for energies close to the Fermi energy is different, at the Fermi energy $\delta A(\varepsilon_F, 0) = \delta A(\varepsilon_F, \pi)$ independently on the radius of the sphere provided that the Fermi level coincides with one of the one-electron levels. An alternative approximate procedure is to express the conduction-electron propagators in terms of the impurity propagator $G_i(\omega)$ and then use for $G_i(\omega)$ a Lorentzian peak at the Fermi energy with a width given by the Kondo temperature T_K .⁴ However, in this procedure $G_i(\omega)$ does not account for the structure of the discrete energy levels of the nanoscopic system and the exact results obtained for an isolated small system are not reproduced. This approach is justified only if there is a large broadening of the one-electron levels of the nanoscopic system, a limit in which we expect a smaller and more diffuse mirage.

These results validate some previous results where the Kondo resonance is not fully self consistently calculated and the many body effects are taken into account in a rather phenomenological way. In addition our results show that also for IV impurities, with a large hybridization or a small E_d , the mirage in the spectral density is still obtained. Another very interesting feature concerns the spin correlations in these systems. We start by presenting the static spin correlation $\langle \mathbf{S}_{imp} \cdot \sigma(\theta, \varphi) \rangle$ where \mathbf{S}_{imp} is the impurity spin operator, $\sigma(\theta, \varphi)$ is the conduction electron spin operator at coordinates (θ, φ) and the brackets indicate the expectation value at the ground state. For a small hybridization the results presented in Figure (3a) clearly show an antiferromagnetic correlation for small θ resulting from the screening of the impurity spin by the conduction electrons. As θ grows, the spin-spin correlation decreases, however, at the empty focus it increases again giving rise to a magnetic mirage. At the empty focus, the conduction electron spin is fluctuating coherently with the impurity spin as if the Kondo impurity were in its neighborhood. When the Fermi energy coincides with one of the one electron levels, the Kondo effect takes place and the conduction electron spin at the empty focus is always antiferromagnetically correlated with the impurity spin. For the case of a closed shell, the spin-spin correlations are weaker and at the empty focus the conduction electron spin is ferromagnetically correlated with the impurity spin. For a large hybridization charge fluctuations are important and although the local ($\theta = 0$) spin-spin correlations are large the magnetic mirage is not well defined (dashed line in Fig. (3a)).

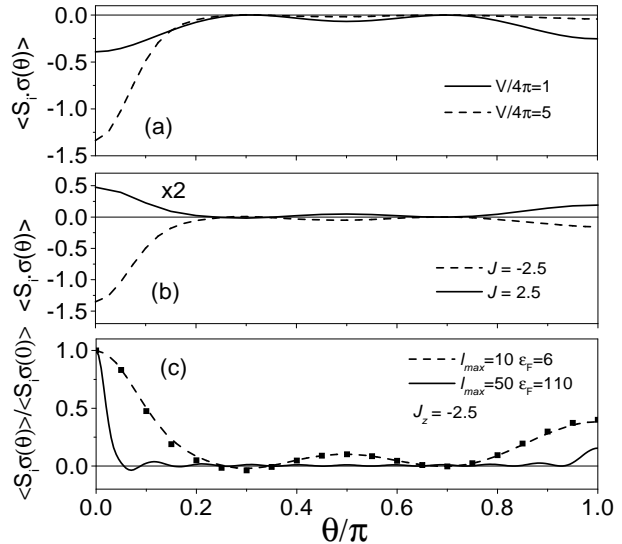


FIG. 3. Spin-spin correlations as a function of θ . (a) Anderson Hamiltonian (1); (b) Kondo Hamiltonian (2) with ferromagnetic and antiferromagnetic coupling J ; (c) Ising-type interaction normalized to the value at $\theta = 0$ for a small (dashed) and large (continuous line) system. Squares are the exact results obtained in the full Hamiltonian (2).

In the Kondo regime the Anderson Hamiltonian can be approximated by the Kondo Hamiltonian which describes correctly the spin dynamics of the system¹²:

$$H = \sum_{l,m,\sigma} \varepsilon_l c_{lm\sigma}^\dagger c_{lm\sigma} + J \mathbf{S}_{imp} \cdot \sigma(0,0) \quad (2)$$

here $J > 0$ is the antiferromagnetic coupling between the impurity and the conduction electron spins. For $J < 0$, this Hamiltonian describes the effect of a magnetic non-Kondo impurity with a ferromagnetic (FM) sd -coupling¹¹. We have also calculated the spin correlations for a magnetic non-Kondo impurity with FM coupling to the conduction electrons. The results obtained for $J > 0$ and $J < 0$ are compared in Fig. (3b). The spin correlation at short distances (small θ) are larger for the Kondo impurity. This is due to the singular nature of the Kondo scattering which is not obtained for a ferromagnetic sd -coupling. The magnetic mirage is proportionally more pronounced for the latter case where perturbations or simple approximations can be used to estimate the spin-spin correlations. For the $J < 0$ we have calculated the correlations with an Ising-type interaction $J_z S_{imp}^z \sigma^z(0,0)$ and, as shown in Fig. (3c), the results quantitatively reproduce the exact results obtained with the full Hamiltonian (2). This allows us to use, for the case $J < 0$, the Ising-type interaction to estimate the spin correlations in much larger systems and in more complicated geometries. The spin correlations obtained for a large sphere are also shown in Fig. (3c). The magnetic mirage is quite pronounced and despite the fact that the two foci can be even further than 50 interatomic distances, the spin cor-

relation for electrons at the empty focus are as large as the correlations at distances of the order of one or two interatomic distances from the occupied focus.

A systematic analysis of the behavior of the magnetic mirage can be made by changing the sphere radius R and keeping the electron density constant. As the radius increases, the characteristic energy difference δE between two consecutive one-electron levels decreases and for some particular values of R the Fermi level coincides with one of the one-electron states. We analyzed these cases in which there is an open (non-filled) shell in the sphere. The results obtained for different radii are presented in Fig. (4), the inset shows the amplitude of the spin-spin correlation between the impurity spin and the conduction electron spin at the empty focus for fixed density (same as in Fig. 1) and $J_z = 0.25$ as a function of R . At short distances ($\theta \approx 0$) the spin-spin correlation is sensitive to both, the system size and the cutoff l_{\max} and as θ increases it becomes independent of l_{\max} . At the empty focus two different regimes can be observed: For small systems, the level spacing δE is smaller than J_z and the impurity polarizes the electron at the Fermi level; the magnetization profile is essentially given by the one-electron wave function $|Y_{l_F, m=0}(\theta)|^2$ where l_F is the Fermi angular momentum. Since these wave functions at $\theta = \pi$ increase as l_F increases, the magnetic mirage increases with R for small systems. For large systems, $\delta E \ll J_z$, the impurity produces a mixing of states with different l that interfere destructively and the magnetic mirage tends to zero as R goes to infinity.

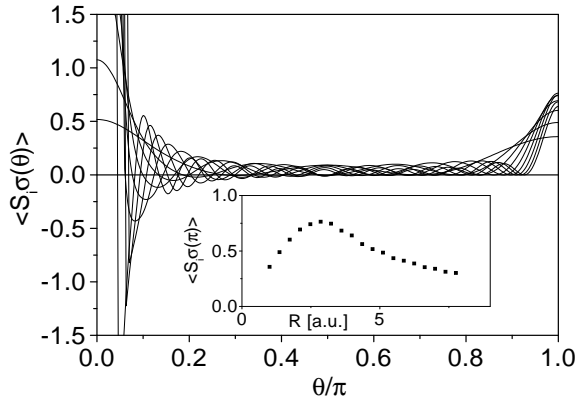


FIG. 4. Spin-spin correlations vs θ for the Ising limit for different R with fixed J_z and electron density (open shell). Inset: Spin correlation at $\theta = \pi$ as a function of R for the same J_z

As a consequence of the presence of the magnetic mirage, we can infer that if an additional impurity is placed at the empty focus (i.e. when there are two impurities in the system, one at each focus), they will strongly interact. In this case the impurity-impurity coupling is ferromagnetic if the Fermi level lies close to one of the energy levels of the nanoscopic system and is antiferromagnetic

and much weaker if the Fermi energy lies between two one-electron levels. Results obtained for the magnetic mirage in the elliptic quantum corral will be presented elsewhere.

In summary, we have presented here an exact many body calculation for impurities in nanoscopic systems with focusing properties. The spectroscopic characteristics of the Kondo impurity, which are always observed in its neighborhood for open shell systems, are reproduced at the opposite point on the sphere giving rise to a spectroscopic mirage of the impurity. Our results also show that impurities with a large hybridization, which induces large charge fluctuations, also give rise to spectroscopic mirages. This may be important since ab-initio calculations of Co on noble metal surfaces indicate that charge fluctuations are relevant for these systems¹³. We compared the exact results for the Kondo impurity with those obtained with an effective model which includes a resonant state at the Fermi level. Although there are some quantitative differences between the two models, the exact results are qualitatively reproduced by the simple one-body approach. We have also calculated the exact spin-spin correlations in small systems. The results show the existence of magnetic mirages: at the empty focus conduction electron spins are fluctuating coherently with the impurity spin. These magnetic mirages are also obtained for non-Kondo magnetic impurities which couple ferromagnetically with conduction electron spins. For this case the magnetic mirage is more pronounced than for the Kondo impurity.

The results obtained here for a sphere can be extended to other systems with focusing properties such as quantum corrals. In particular, in addition to a mirage in the localized density of states, a magnetic mirage should be observed in such systems in the presence of a Kondo (or sd) impurity. Results for the elliptical corral will be presented elsewhere.

This work was done under PICT grant N02151 (AN-PCYT). K.H. and C. B. are fellows of the Consejo Nacional de Investigaciones Científicas y Técnicas (CONICET).

-
- ¹ H. C. Manoharan, C. P. Lutz, and D. M. Eigler, *Nature* **403** 512 (2000)
 - ² J. Li, W. D. Schneider, R. Berndt and B. Delley, *Phys. Rev. Lett.* **80**, 2893 (1998)
 - ³ V. Madhavan, W. Chen, T. Jamneala, M. F. Crommie and N. S. Wingreen, *Science* **280**, 567 (1998)
 - ⁴ O. Agam and A. Schiller, cond-mat/0006443
 - ⁵ M. Weissmann and H. Bonadeo, cond-mat/0007485
 - ⁶ D. Porras, J. Fernández-Rossier and C. Tejedor, cond-mat/0007445

- ⁷ G. F. Fiete et al, cond-mat/0008170
- ⁸ A. A. Aligia, cond-mat/0101082
- ⁹ E. Dagotto and A. Moreo, Phys. Rev. D **31**, 865 (1985)
- ¹⁰ E. R. Gagliano and C. A. Balseiro, Phys. Rev. Lett, **59**, 2999 (1987)
- ¹¹ P. W. Anderson, Phys. Rev. **124**, 41 (1961)
- ¹² J. R. Schrieffer and P. A. Wolff, Phys. Rev. **144**, 491 (1966)
- ¹³ M. Weissmann and A. Saul, Phys. Rev. B **59**, 8405 (1999)